Science Advances
AAAS

Supplementary Materials for

Imaging and tracing the pattern of adult ovarian angiogenesis implies a strategy against female reproductive aging

Xueqiang Xu, Lu Mu, Lingyu Li, Jing Liang, Shuo Zhang, Longzhong Jia, Xuebing Yang, Yanli Dai, Jiawei Zhang, Yibo Wang, Shudong Niu, Guoliang Xia, Yunlong Yang, Yan Zhang, Yihai Cao, Hua Zhang*

*Corresponding author. Email: huazhang@cau.edu.cn

Published 12 January 2022, *Sci. Adv.* **8**, eabi8683 (2022)
DOI: 10.1126/sciadv.abi8683

The PDF file includes:

Figs. S1 to S9
Legends for movies S1 to S4

Other Supplementary Material for this manuscript includes the following:

Movies S1 to S4

Extended data figures and figure legends:

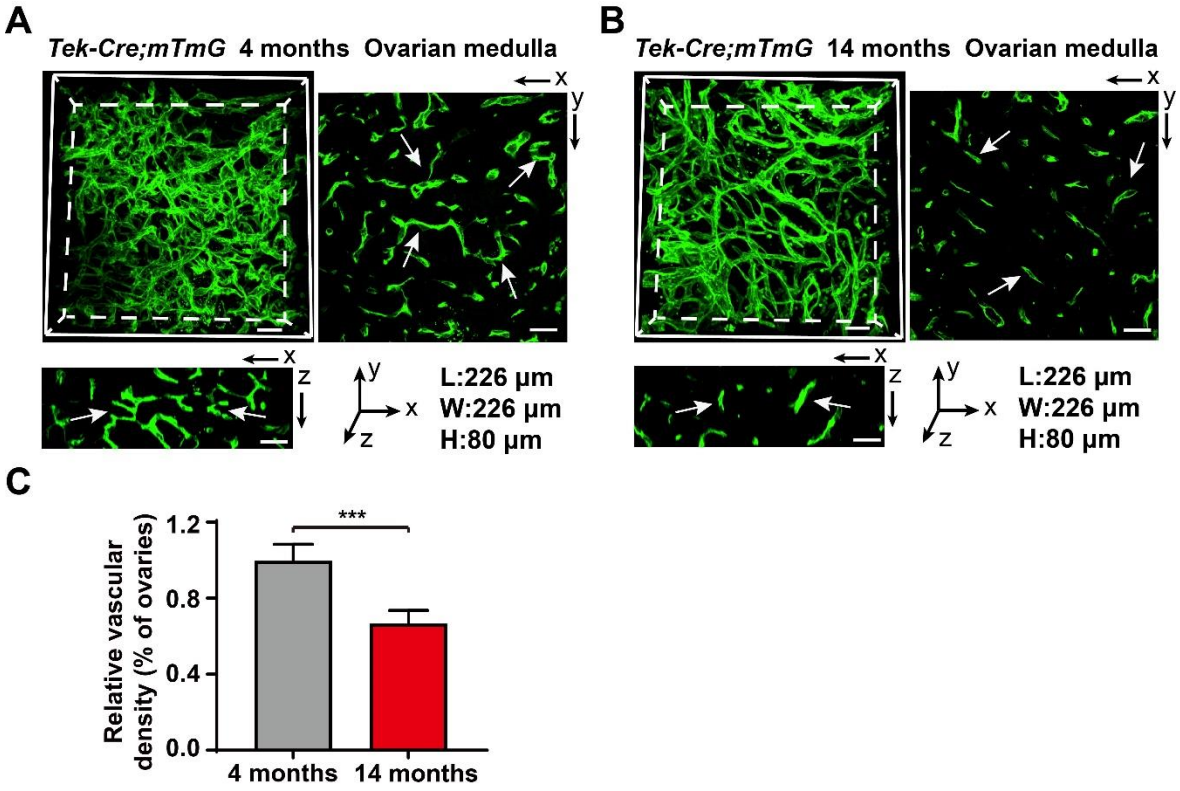

Fig. S1. The density of ovarian blood vessels decreased with aging. (**A-B**) Reconstructed imaging showing a significantly decreased density of GFP labeled blood vessels at 14 months (B) compared to that at 4 months (A). (**C**) Quantification of the relative changes of ovarian blood vessel density (n = 8 ovaries per group). The data are presented as means ± SD. The data were analyzed by a 2-tailed unpaired Student's *t-test*; *** $p < 0.001$. Scale bars: 25 µm (A and B).

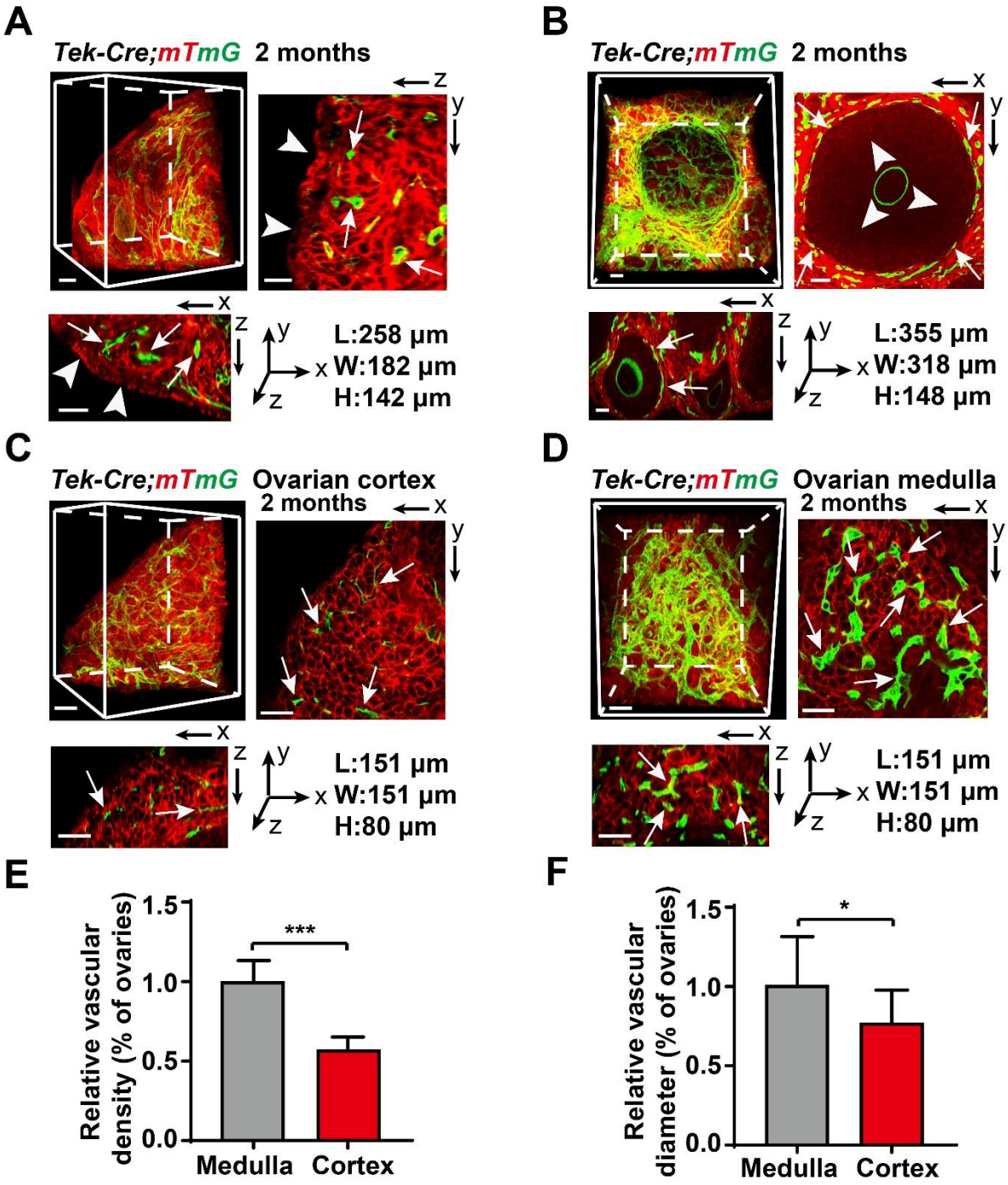

Fig. S2. Analyzing the distributing features of vascular network in the adult ovary. After imaging and reconstruction of 3D vascular network of ovaries, the imaging was cut by Imaris software, and the 3D distribution of blood vessels were detected. (**A**) Showing that blood vessels distribute in the stromal region (arrows) of ovary at 2 months old, but not in the surface epithelium (arrowheads). (**B**) Showing the distributions of blood vessels in the follicle of ovary at 2 months old. Abundant blood vessels were

surrounding the follicles in the theca layer (arrows), but no blood vessels grown to the inside of healthy follicles (arrowheads). (**C**-**D**) The density of blood vessels was significantly higher in the medulla stromal region (D) than that in the ovarian cortical area (C). (**E**) Quantification of vascular density in medulla and cortical area of the ovaries (n = 8 ovaries per group). (**F**) Quantification of the average vascular diameter in medulla and cortical area of the ovaries (n = 8 ovaries per group). The data are presented as means ± SD. The data were analyzed by a 2-tailed unpaired Student's *t-test*; *** $p < 0.001$, * $P < 0.05$. Scale bars: 25 μm (A-D).

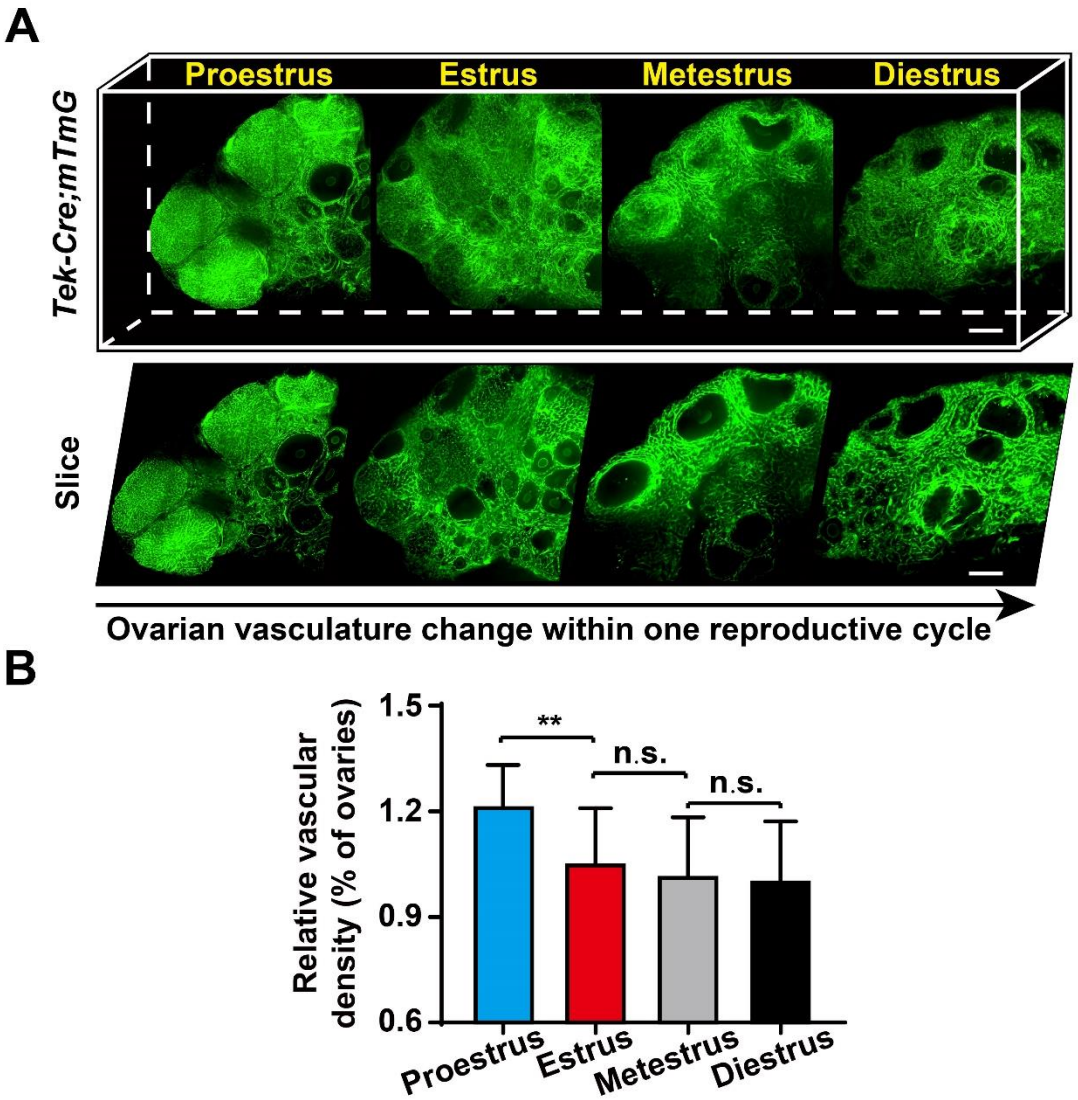

Fig. S3. Analyzing the changing profiles of blood vessels during estrus cycle with high-resolution 3D ovarian imaging. (**A**) Imaging of 3D blood vessels in ovaries at different stages of estrus cycle, showing a higher density of blood vessels in proestrus period. (**B**) Quantification of vascular density at different stages of estrus cycle (n = 8 ovaries per group). The data are presented as means ± SD. The data were analyzed by a 2-tailed unpaired Student's *t-test*; ** $P < 0.01$, n.s. $P \geq 0.05$. Scale bars: 200 μm (A).

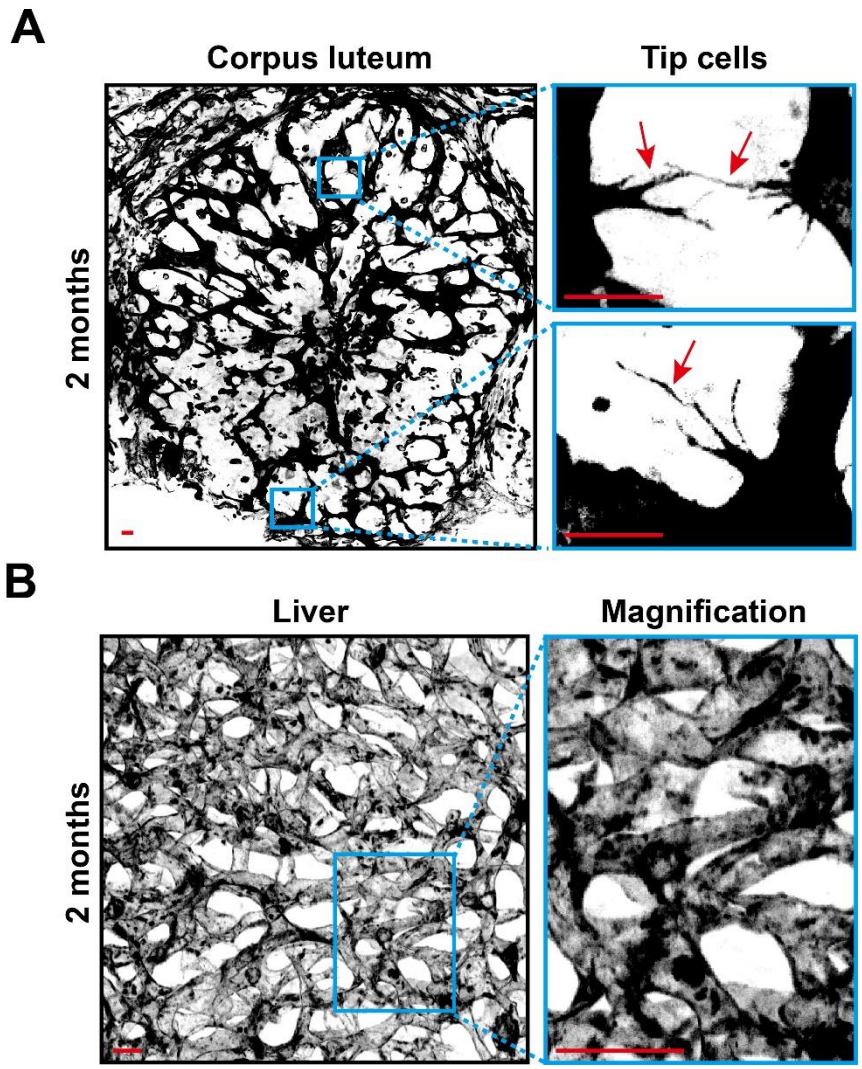

Fig. S4. Imaging and analysis of tip cells in the ovary and liver. (A) Identification of angiogenesis marker cell, the tip cells (arrows), in the CL of ovary at 2 months of age, showing active angiogenesis occurred in the CL. (B) Images of the blood vessels in liver of *Tek-Cre;mTmG* females at 2 months of age. The blood vessels in the adult liver exhibited a smooth surface with no tip cells. Scale bars: 10 μm (A and B).

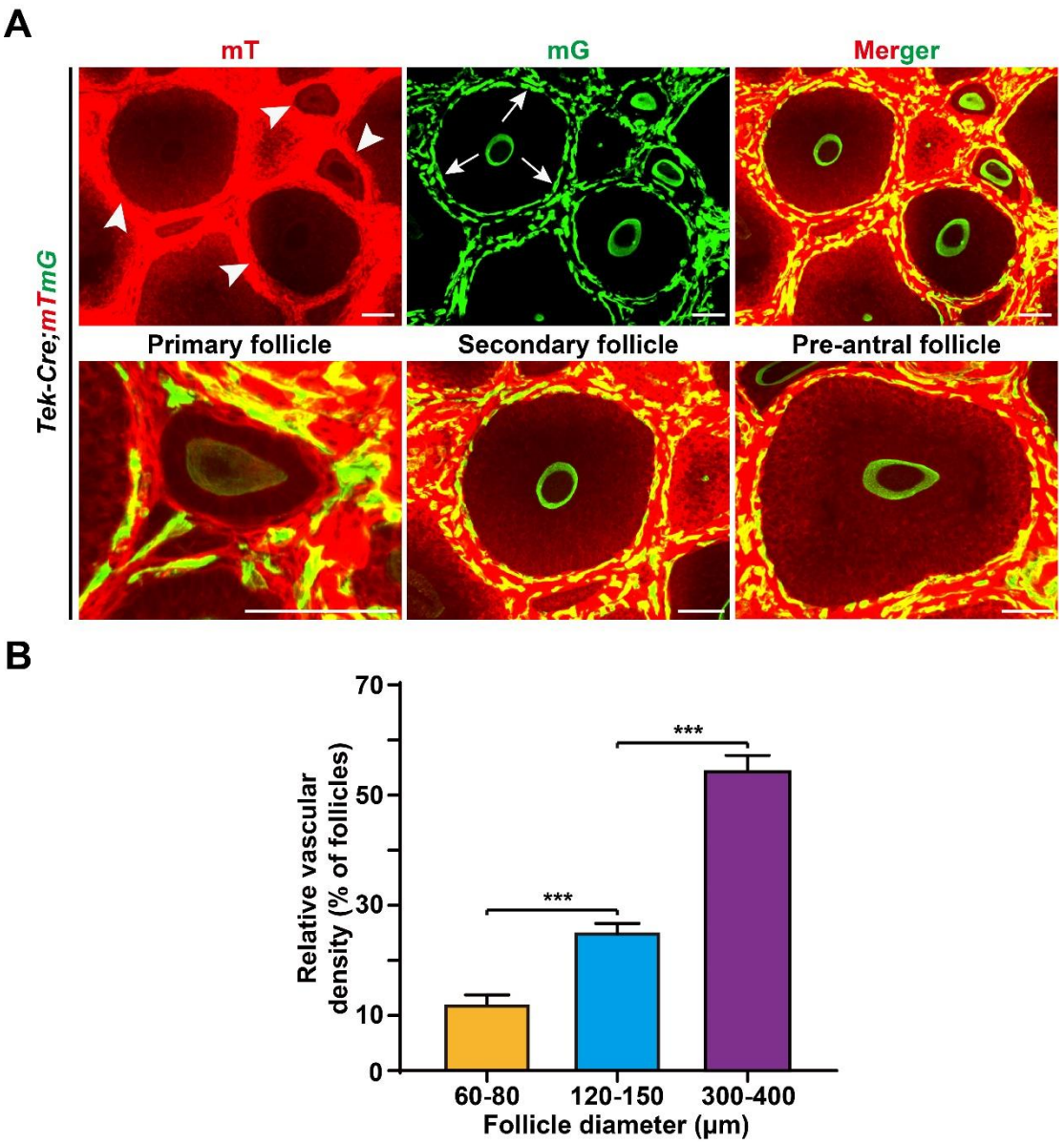

Fig. S5. Identification of follicle developmental stages and quantification of the vascular density in high-resolution imaging of *Tek-Cre;mTmG* ovaries. (A) The stages of growing follicles were identified by the mT labeled morphology (arrowheads) in single optical section of *Tek-Cre;mTmG* ovaries, whereas the blood vessels were detected by mG (arrows). (**B**) After 3D imaging, the capillary density of individual follicle was analyzed in *Tek-Cre;mTmG* ovaries at 2 months. The statistical analysis showed that a significant increase of blood vessel density with follicle development (n = 15 for each stage). The data are presented as means ± SD. The data were analyzed by a 2-tailed unpaired Student's *t-test*; *** $p < 0.001$. Scale bars: 50 μm (A).

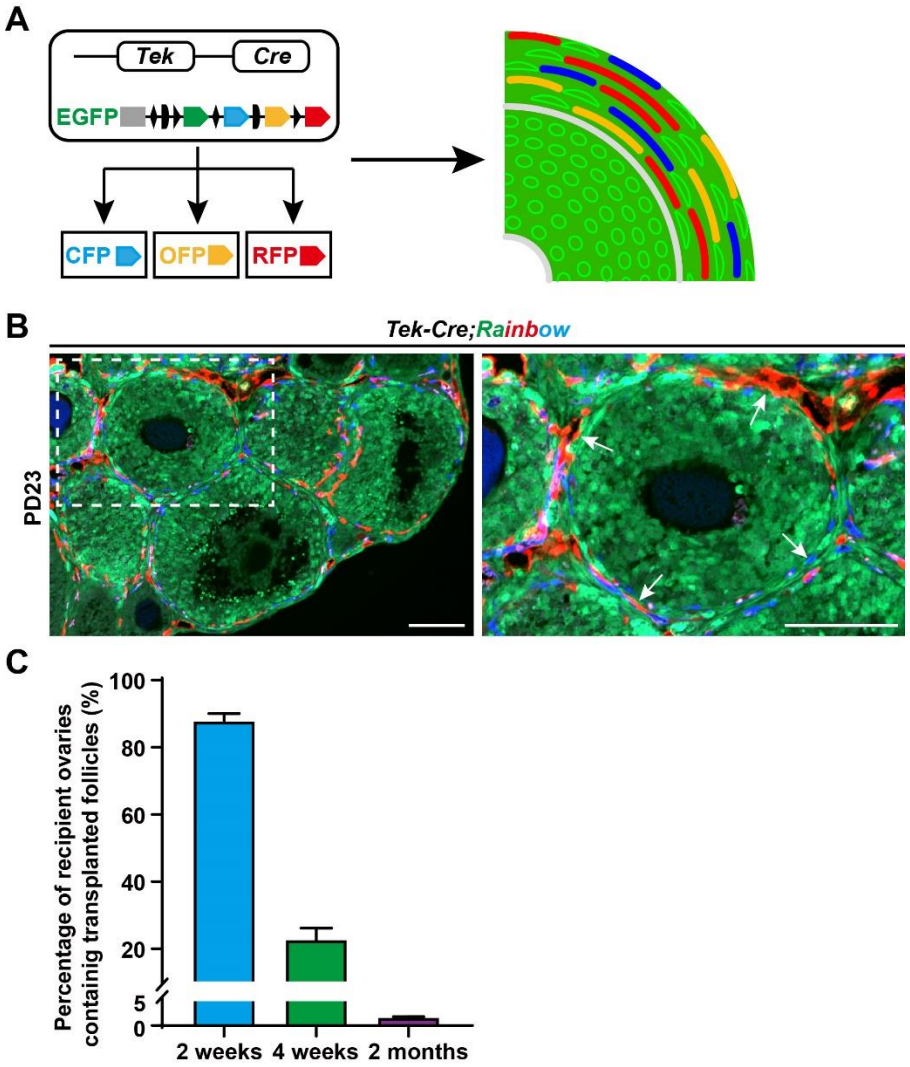

Fig. S6. Tracing the developmental fate of follicle blood vessels by *Tek-Cre;Rainbow* mice. (**A**) Schema of the labeling strategy of endothelial cells in *Tek-Cre;Rainbow* mice. The green fluorescent protein (EGFP) was randomly replaced by RFP, OFP or CFP in the *Tek*-positive endothelial cells in the animals. (**B**) Multi-fluorescent endothelial cells (arrows) in the ovaries of *Tek-Cre;Rainbow* female at PD23. (**C**) The ratio of recipient's ovaries with donor follicles at different time points after transplantation. Scale bars: 50 μm (B).

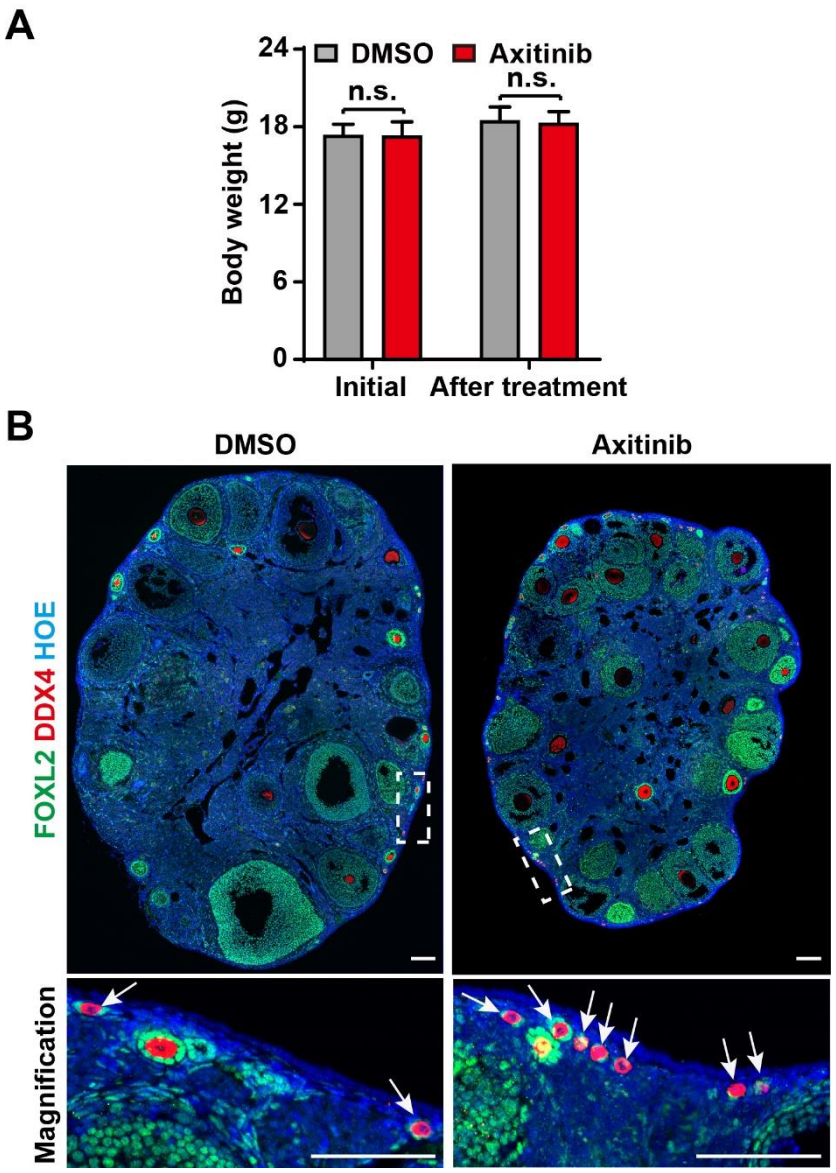

Fig. S7. Axitinib treatment kept the follicle reserve in ad ult females. (**A**) During the treatment, an identical increase of body weight in the Axi and control groups. (**B**) Immunostaining for granulosa cells (FOXL2, green) and oocytes (DDX4, red) in ovarian sections showing the distribution of PF (arrows) in the cortical region of ovaries after 1 month treatment with or without Axi. Abundant PFs were observed in the ovarian cortex of Axi group. The data are presented as means ± SD. The data were analyzed by a 2-tailed unpaired Student's *t-test* and n.s. $P \geq 0.05$. Scale bars: 100 μm (B).

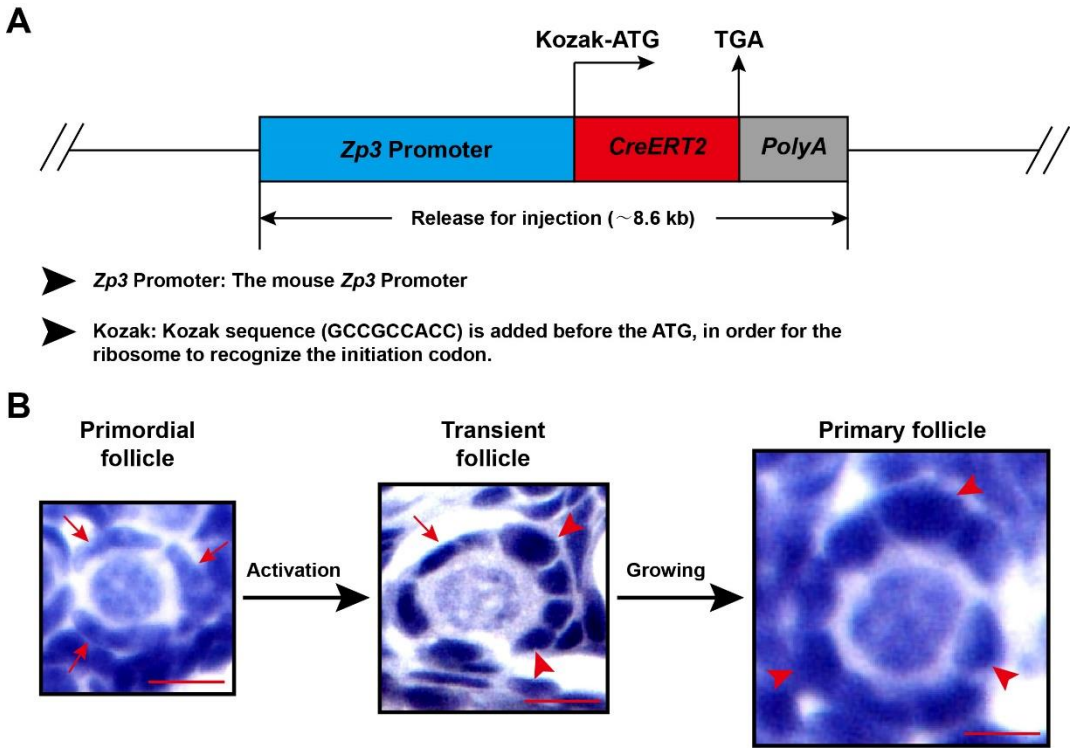

Fig. S8. Construction of *Zp3-CreER*^{T2} mice and the morphological transformation of primordial follicle during activation. (**A**) The schematic diagram of *Zp3-CreER*^{T2} mice. The *Zp3-CreER* knock-in mouse line was generated by inserting the *CreER*^{T2} into the frame after *Zp3* promoter in the *Zp3* gene. (**B**) The histological difference of primordial, transient and primary follicles in the ovary. The PFs were identified by surrounding with flatten pre-granulosa cells (preGCs) (arrows) in the ovaries. After activation, the transient follicles were surrounded by a mixed preGCs and cuboidal granulosa cells (GCs) (arrowheads), and all preGCs transferred to GCs in the primary follicles. Scale bars: 10 μm (B).

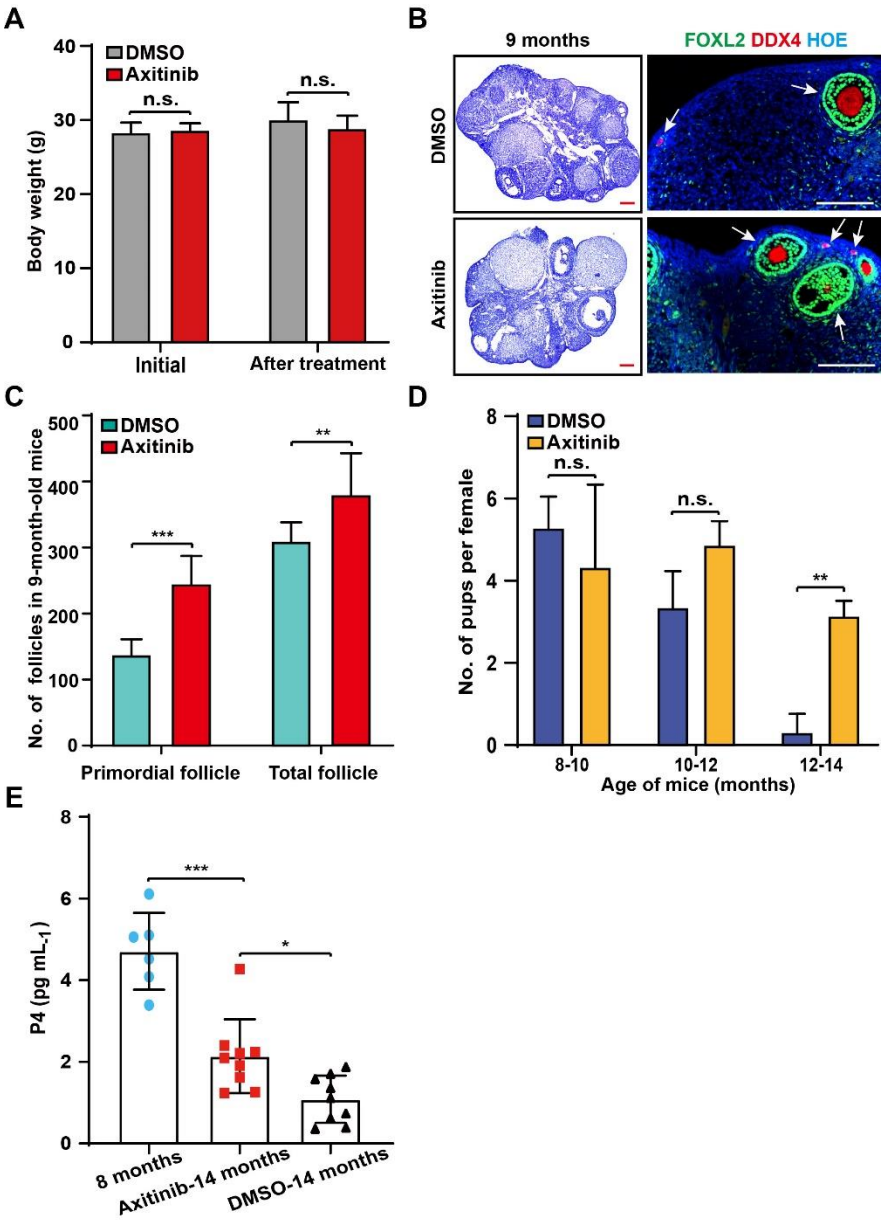

Fig. S9. Appropriate inhibition of adult angiogenesis extends the reproductive lifespan of aged females. (**A**) An identical increase of body weight in the Axi and control groups during the period of treatment. (**B**) Histological analysis showed a normal general morphology of ovaries after 1 months of Axi treatment. (**C**) Follicle counting results showed significantly increased number of both PFs and total follicles was found in Axi treated ovaries compared to controls ($n \geq 6$). (**D**) Average number of pups per female during different reproductive period at 8-10, 10-12 and 12-14 months of age in Axi and control groups. (**E**) At 14 months, the P4 level of female mice in the Axi treatment group was significantly higher than that in the control group. The data are presented as means ± SD. The data were analyzed by a 2-tailed unpaired Student's *t-test* and *** $P < 0.001$, ** $P < 0.01$, * $P < 0.05$, n.s. $P \geq 0.05$. Scale bars: 100 μm (B).

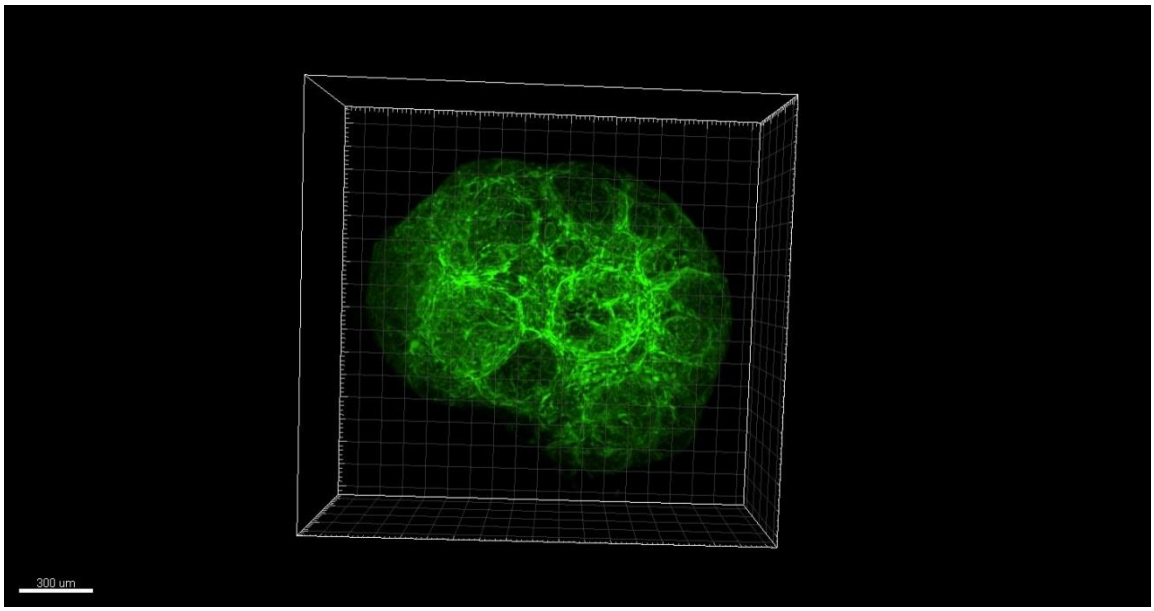

Movie S1. High-resolution, volumetric imaging of *Tek-Cre;mTmG* ovarian vessels after clearing. Three-dimensional reconstruction showing the distributing profile of vascular structures in the ovaries of *Tek-Cre;mTmG* females. The rotary 3D movie was processed by Imaris software. The scale bars change as views in the movie. (See Movie S1.mov)

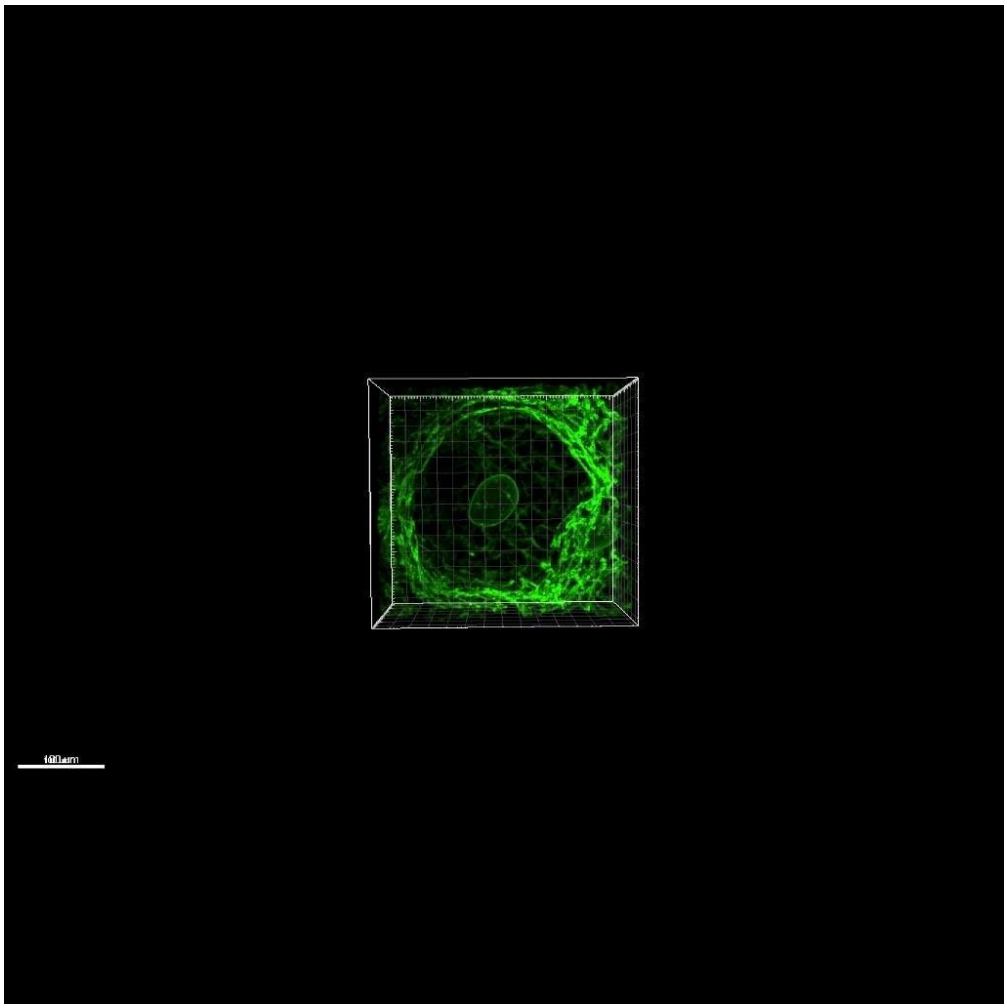

Movie S2. Three-dimensional reconstruction showing the follicle capillary in *Tek-Cre; mTmG* ovary. Three-dimensional reconstruction of the vascular structures in the ovaries from *Tek-Cre;mTmG* ovary. The movie shows that the follicular capillaries present a reticular structure surrounding the follicles. The rotary 3D movie was processed by Imaris software. The scale bars change as views in the movie. (See Movie S2.mov)

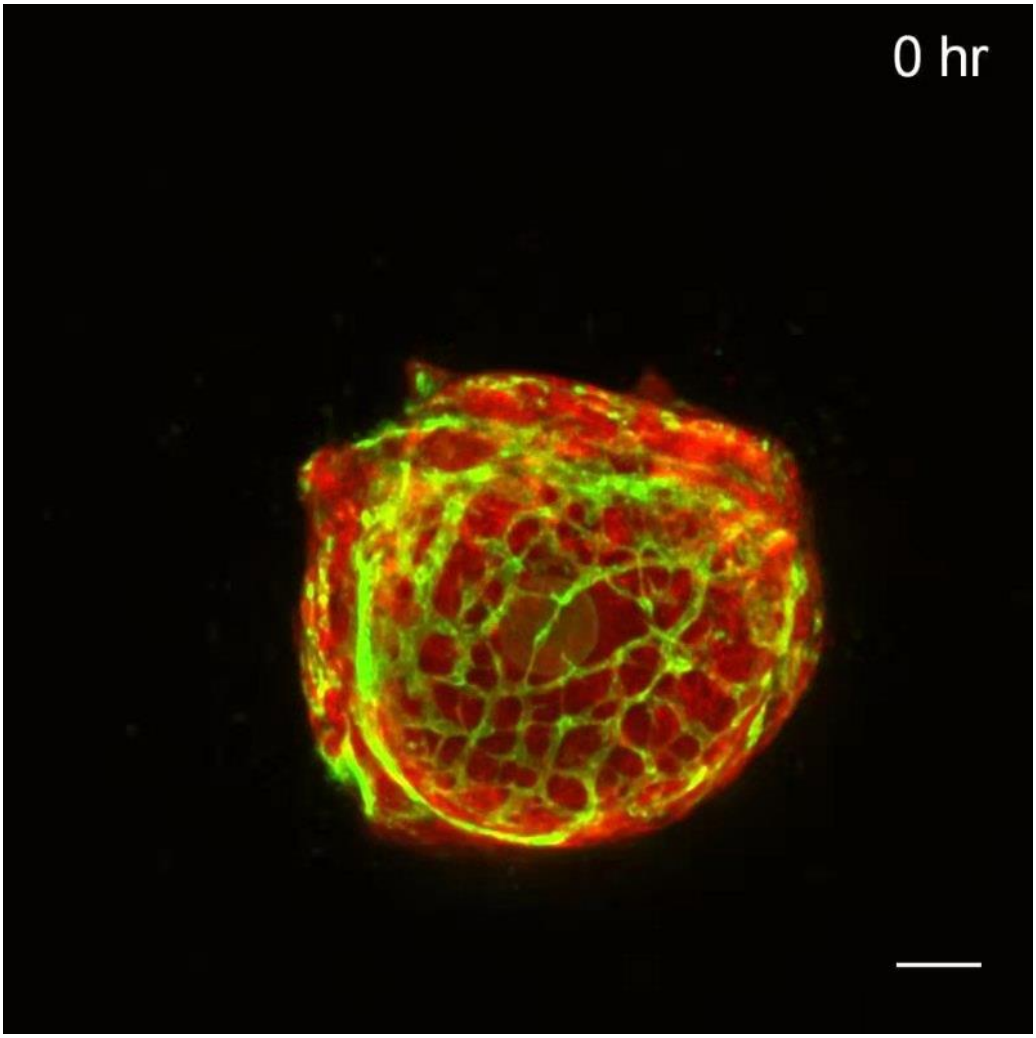

Movie S3. Time-lapse fluorescence observation showing the formation of the follicular vascular network. Time-lapse imaging of living follicle from *Tek-Cre;mTmG* females showing the dynamic change of the follicular vascular network during 24 h observation, dramatic branching and extension of mG labeled blood vessels were observed. Scale bars: 50 μm. (See Movie S3.mov)

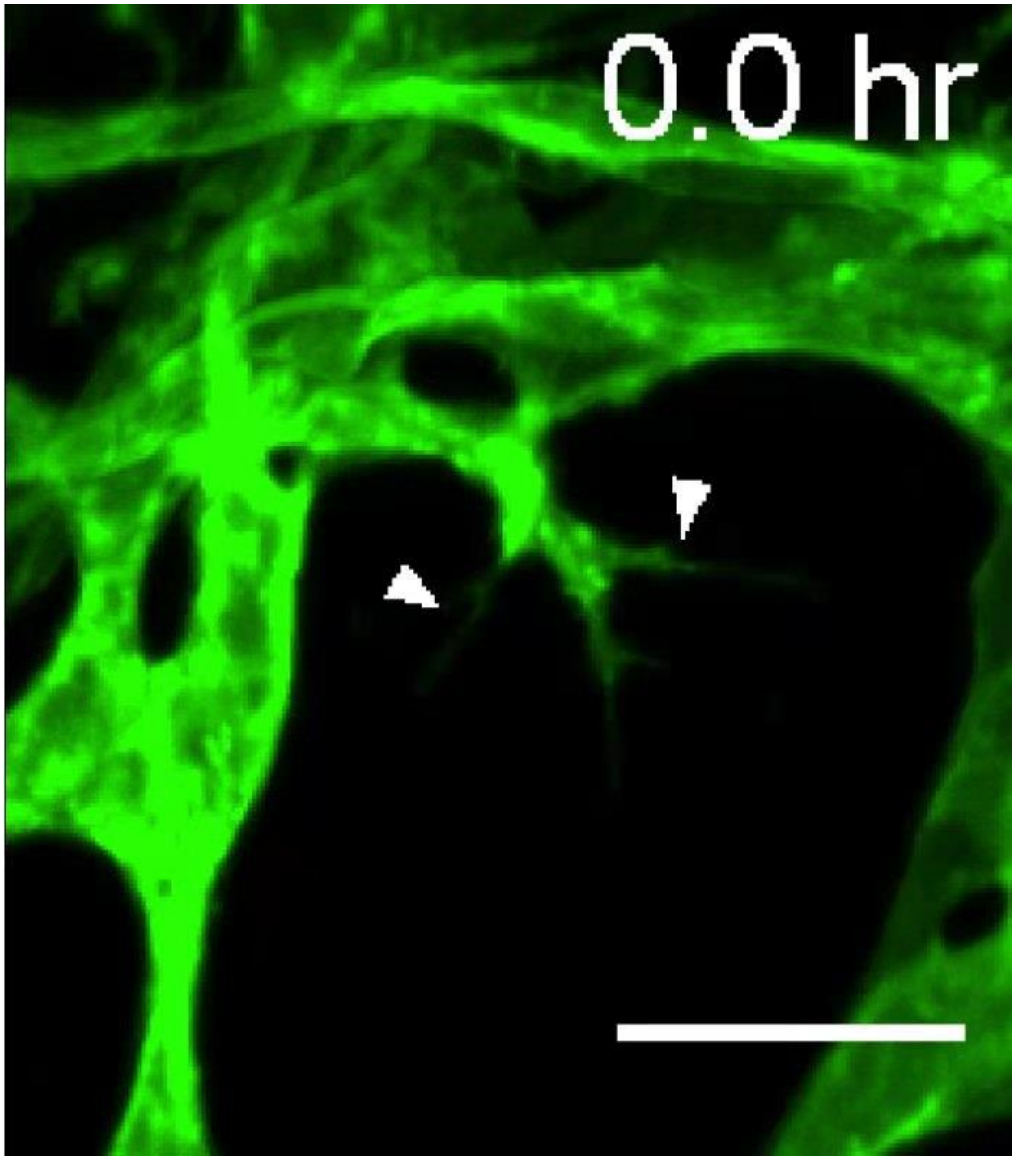

Movie S4. Time-lapse observation the fusion of the tip cells. Time-lapse imaging of living follicular vessels from *Tek-Cre;mTmG* females clearly showed that expanded vascular endothelial cells form new blood vessels through TP fusion, thus building a complete vascular network on the follicle. Scale bars: 25 μm. (See Movie S4.mov)